AGU PUBLICATIONS

Water Resources Research

RESEARCH ARTICLE
10.1002/2013WR014944

Key Points:
- Hydrologic turnover is induced by gains and losses along a stream network
- Watershed and network shape create distinct patterns of hydrologic turnover
- Hydrologic turnover modifies watershed signals

Correspondence to:
J. Mallard,
mallard.john@gmail.com

Citation:
Mallard, J., B. McGlynn, and T. Covino (2014), Lateral inflows, stream-groundwater exchange, and network geometry influence stream water composition, *Water Resour. Res.*, *50*, 4603–4623, doi:10.1002/2013WR014944.

Received 22 OCT 2013
Accepted 19 MAR 2014
Accepted article online 25 MAR 2014
Published online 5 JUN 2014

Lateral inflows, stream-groundwater exchange, and network geometry influence stream water composition

John Mallard[1], Brian McGlynn[1], and Tim Covino[2]

[1]Nicholas School of the Environment, Duke University, Durham, North Carolina, USA, [2]Ecosystem Science and Sustainability, Natural Resource Ecology Lab, Colorado State University, Fort Collins, Colorado, USA

Abstract The role of stream networks and their hydrologic interaction with hillslopes and shallow groundwater in modifying and transporting watershed signals is an area of active research. One of the primary ways that stream networks can modify watershed signals is through spatially variable stream gains and losses, described herein as hydrologic turnover. We measured hydrologic gain and loss at the reach scale using tracer experiments throughout the Bull Trout watershed in the Sawtooth Mountains of Idaho. We extended the results of reach scale experiments to the stream network using empirical relationships between (1) watershed area and stream discharge and (2) stream discharge and percent stream water loss to the groundwater system. We thus incorporate linkages between (1) hillslopes and stream networks via lateral inflows and (2) stream networks and shallow groundwater via hydrologic exchange. We implemented these relationships within a concise analytical framework to simulate hydrologic turnover across stream networks and estimate the variable influence exerted by upstream reaches and streamflow source locations on stream water composition across stream networks. Application to six natural Sawtooth watersheds and seven synthetic watersheds with varying topographic structure and stream network geometry indicated that contributions to discharge from any upstream source depend on the magnitude of the initial input, but also on the distribution of hydrologic turnover occurring along the stream network. The evolution of stream water source compositions along stream networks was unique in each watershed due to the combination of watershed structure and stream network geometry. Our results suggest that a distributed representation of hydrologic turnover at the stream network scale can improve understanding of how the stream network can modify source water compositions along the stream.

1. Introduction

Stream networks are integral components of watersheds. They integrate, transform, and transmit watershed physical [*Kirchner*, 2009; *Robinson et al*., 1995; *Rinaldo et al*., 1995; *Rodríguez-Iturbe and Valdés*, 1979] and biogeochemical [*Ensign and Doyle*, 2006; *Fisher et al*., 2004; *Vannote et al*., 1980] process signatures. They are positioned within the watershed between hillslopes, shallow groundwater, and downstream waters. As such, they organize interactions between these watershed components. Observing and sampling streams at watershed outlets has provided valuable information for understanding watershed processes and has led to development of the basic tools of watershed hydrology (e.g., the unit hydrograph) [*Sherman*, 1932] and biogeochemistry (e.g., the small watershed concept) [*Bormann and Likens*, 1967]. However, both physical and biogeochemical process signals delivered to streams can be convoluted in watershed outlet observations by stream network and watershed structure, and by spatially heterogeneous hydrologic or biogeochemical processes occurring along the stream network.

Solute signals can be modified by multiple biogeochemical or physical processes. Biogeochemical processes can include nutrient cycling [*Mulholland et al*., 2008] or other types of chemical reactions and processing [*McKnight and Bencala*, 1990]. Furthermore, these processes can occur within streams [*Roberts and Mulholland*, 2007; *Sebestyen et al*., 2008] or their adjacent hyporheic zones, riparian areas, or wetlands [*McClain et al*., 2003]. Physical processes can additionally exert strong influences on the inputs to stream networks from adjacent hillslopes: with either attenuation by dispersive mechanisms acting at the watershed scale or modification by hydrological exchange between reservoirs with distinct biogeochemical signatures and residence times (e.g., shallow groundwater).

Hydraulic and geomorphic processes can induce dispersion. These dispersive processes have been extensively and rigorously studied at the scale of stream networks and can be broadly broken out into three types of dispersion: hydrodynamic, geomorphic, and kinematic. Reach-scale variability in flow velocities, described as hydrodynamic dispersion [*Fisher et al*., 1979; *Rinaldo et al*., 1991; *Snell and Sivapalan*, 1994] induces dispersion within stream reaches. This form of dispersion, however, has been found less important at the watershed scale than geomorphic dispersion [*Rinaldo et al*., 1991] or kinematic dispersion [*Saco and Kumar*, 2002a, 2002b]. The geometry of the stream network induces geomorphic dispersion of signals entering stream networks due to the distribution of flow path lengths across the stream network [*Gupta et al*., 1980; *Kirkby*, 1976; *Lee and Delleur*, 1976; *Rinaldo et al*., 1991; *Rodríguez-Iturbe and Valdés*, 1979; *Snell and Sivapalan*, 1994]. Spatially variable flow velocities within the stream network [*Agnese et al*., 1988; *Yen and Lee*, 1997; *Leopold and Maddock*, 1953] can further disperse an input signal; this form of dispersion is commonly termed kinematic dispersion [*Saco and Kumar*, 2002a, 2002b]. The degree to which each of these forms of dispersion act on stream network input signals varies depending on the basin scale, flow state, and formulation of the problem [e.g., *Botter and Rinaldo*, 2003; *Robinson et al*., 1995]. These metrics of dispersion have been most commonly applied in the context of interpreting or predicting runoff measured at the outlet of the watershed or assessing flood risks via distributions of hydrologic wave travel times through the watershed and therefore generally use wave celerity, rather than particle velocities.

In an effort to understand how both stationary and nonstationary travel time distributions can be used to explain how solutes move through watersheds, recent studies have focused on particle velocities as opposed to wave celerities. Owing to the inherent complexity of fully characterizing inputs and flow paths, studies have usually focused on deconvolving watershed outlet chemical datasets [*McGuire and McDonnell*, 2006]. Because of the challenges in introducing tracers into hillslopes/whole watersheds, studies have leveraged conservative tracers introduced into watersheds by precipitation such as stable water isotopes (^{18}O or ^{2}H) [i.e., *Soulsby et al*., 2000; *Tetzlaff et al*., 2009; *Uhlenbrook et al*., 2002] or chloride (Cl^{-}) [*Benettin et al*., 2013a; *Hrachowitz et al*., 2009; *Kirchner et al*., 2001] to make inferences about how watersheds convolve input signals by physical means (but see Botter et al. 2008 for an exception using conservative and non-conservative tracers). Many of these studies have made the simplifying assumption of stationarity in a watershed's travel time distribution. Recently, extensive progress has been made on theoretical frameworks that facilitate the relaxation of this assumption both theoretically [e.g., *Benettin et al*., 2013b, *Rinaldo et al*., 2011; *van der Velde et al*., 2012] and in application to outlet time series' of conservative tracers [e.g., *Benettin et al*., 2013a]. One strength of these analyses is the integration of the watershed response continuously across that watershed, avoiding a distinction between soil, groundwater, and stream flow paths. However, given that solutes transported through watersheds are subject to heterogeneous physical and biogeochemical settings, and that a crucial distinction is the one between streams and adjacent groundwater [e.g., *Findlay*, 1995], understanding their interaction can aid in interpretation of watershed scale signals.

The interaction between streams and adjacent groundwater has been studied [see *Kalbus et al*., 2006 for methodological review] primarily within the context of hyporheic zone interactions and transient storage [*Bencala and Walters*, 1983; *Harvey et al*., 1996; *Runkel*, 2002; *Wagner and Harvey*, 1997]. Many of these experiments, although performed at the reach scale, have focused on recovered tracer assessment of streamwater-groundwater exchanges over short temporal scales (i.e., minutes to hours) and spatial scales (i.e., centimeters to meters) characteristic of residence time in eddies or the shallow hyporheic zone. However, interaction between streams and adjacent groundwater can occur along a continuum of spatial and temporal scales [*Cardenas*, 2008]. Longer duration and larger spatial scale streamwater-groundwater exchange processes are increasingly being recognized. These studies quantify unrecovered tracer to document that stream reaches not only gain water from or lose water to groundwater, but that dynamic and simultaneous gains and losses can occur across a broad range of flow states and stream reach morphologies on time scales greater than hours and days and spatial scales of tens of meters to kilometers [*Bencala et al*., 2011; *Covino and McGlynn*, 2007; *Covino et al*., 2010, 2011; *Payn et al*., 2009; *Ruehl et al*., 2006; *Ward et al*., 2013]. This bidirectional movement of water into and out of streams can influence stream solute composition because streams can lose water of one biogeochemical signature and gain water of another [*Covino and McGlynn*, 2007; *Hill*, 1990; *McKnight and Bencala*, 1990; *Mulholland and DeAngelis*, 2000]. Most of these studies focus on reach-scale measurements; however, the serial organization of streams means that these processes can compound with even more significant implications at larger scales [i.e., *Wondzell*, 2011]. It can be expected that relationships between larger scale streamwater-groundwater exchange and

watershed or channel morphology would exist in many systems [*Leopold et al*., 1964]. To this end, recent studies have utilized spatially distributed measurements across stream networks to characterize streamwater-groundwater exchange heterogeneity and make inferences at the stream network scale [*Briggs et al*., 2010; *Covino et al*., 2011]. Extension of measurements necessarily made at the reach scale to full stream networks can provide insight into how stream network geometry and watershed structure can organize patterns of stream exchange at the network scale and manifest in observed dynamics at watershed outlets.

The longitudinal distribution of dynamic stream gains and losses along a stream network can be influenced by watershed structure. Watershed structure is defined here as the arrangement of hillslope convergence and divergence and the resulting spatial pattern of upslope accumulated area [*Jencso et al*., 2009]. It has long been recognized that the magnitude of water input to streams can be related to the amount of lateral watershed area or size of the adjacent hillslope [*Anderson and Burt*, 1978; *Beven and Kirkby*, 1979]. Many studies have related watershed dynamics, either explicitly or implicitly, to the unique distributions of flow paths within the watershed as a whole or within those watersheds' hillslopes [e.g., *Emanuel et al*., 2013; *Jencso and McGlynn*, 2011; *Kirchner et al*., 2000; *McDonnell et al*., 1991; *McGlynn and Seibert*, 2003; *McGlynn et al*., 2004; *McGuire et al*., 2005; *Nippgen et al*., 2011; *Weiler et al*., 2003]. Studies have also used hillslope response functions or other characterizations of hillslope transport together with, for example, geomorphic instantaneous unit hydrograph (GIUH) analyses [e.g., *D'Odorico and Rigon*, 2003; *Mesa and Mifflin*, 1986; *Naden*, 1992; *Saco and Kumar*, 2004; *van der Tak and Bras*, 1990; *Woods and Sivapalan*, 1997]. This integration of hillslope effects and stream network geometry facilitates understanding how whole watersheds modulate runoff or biogeochemical signals, while explicitly incorporating the distinction between terrestrial watershed and stream network processes.

Stream network geometry determines the distribution of distances water and solutes travel from input to the stream to the watershed outlet. This distribution of stream network travel distances was introduced as the distribution of "width" by *Kirkby* [1976] and is commonly referred to as the width function. This characterization of stream networks is commonly used to interpret and predict how stream networks modulate hydrologic signals [e.g., *Lee and Melleur*, 1976] within the context of the geomorphologic instantaneous unit hydrograph (GIUH) [*Rodriguez-Iturbe and Valdes*, 1979]. When considering dynamic hydrologic exchange between streams and groundwater, stream network geometry is important because, among other reasons, it organizes dynamic, reach-scale gains, and losses to and from streams. Because streams are serially organized flow systems [e.g., *Stanford and Ward*, 1993], stream observations of biogeochemical signals are the product of cumulative processing longitudinally along the entire stream network. This processing occurs at the stream network and is the result of connections between hillslopes, the stream network, and shallow groundwater. Therefore, the stream source composition evolves through a stream network to reflect inputs, exchange, and processing along that network. Here we define stream source composition as the distribution of upstream water sources at a given location within the stream network. We use the word "source" to refer to the location in the network where water most recently entered the stream network. We suggest that watershed structure and stream network geometry exert a combined influence on the longitudinal evolution of these compositions due to their influence on the organization of serial stream gains and losses.

Stream gains and losses to and from groundwater that vary along a stream network can lead to modification of stream source composition, and therefore of signals delivered to the stream network from the watershed, moving downstream. This process of simultaneous gains and losses and the resulting downstream evolution of stream water composition is referred to here and in *Covino et al*. [2011] as hydrologic turnover (see section 2 for detailed explanation). *Covino et al*. [2011] introduced a method for extending reach-scale measurements of stream gains and losses to the network scale based on empirical observations and relationships. Their proof of concept modeling results for a single watershed suggested that source water composition was dominated by the organization of local hillslope area in the headwaters but shifted to be more reflective of compounded hydrologic turnover moving in a downstream direction through the stream network. However, that study did not explicitly consider how source water compositions vary across a range of natural and synthetic watersheds due to spatially variable, longitudinally compounded hydrologic turnover through each stream network.

Here we focus on stream network scale hydrologic turnover and how it can manifest as distinct modifications of stream water source composition within unique stream networks under conditions of hydrologic

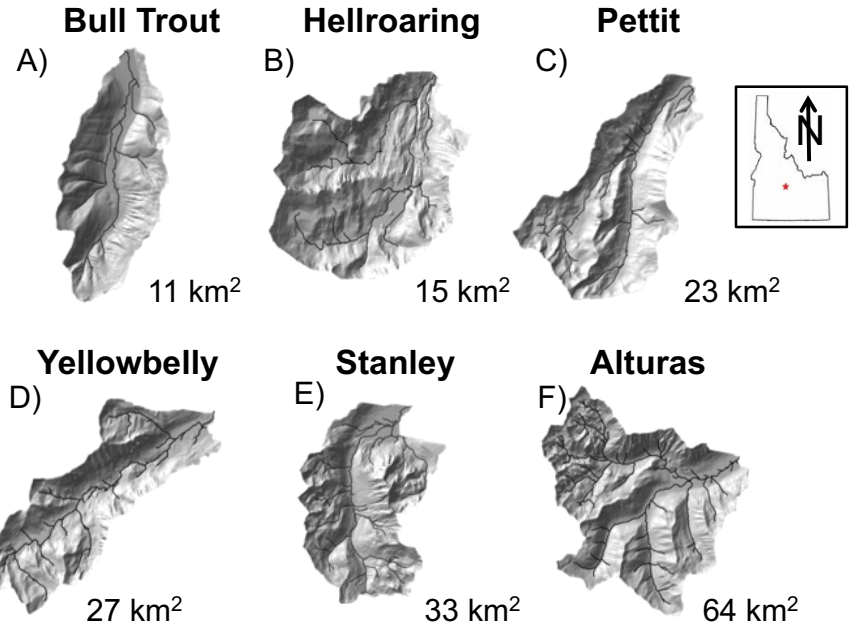

Figure 1. (a–f) Detailed hillshade, stream network, and area for the six watersheds considered in this study. Watersheds are arranged in order of increasing watershed size. Stream networks were delineated based on watershed DEMs using an area accumulation threshold of 20 ha for channel initiation. (Inset) Location of the six watersheds within the Sawtooth Mountains of central Idaho.

equilibrium (e.g., summer base flow in a snowmelt dominated system). We extend the methods and analyses first presented as a partial and preliminarily case study in *Covino et al*. [2011] to include seven synthetic watersheds and six natural watersheds within the Sawtooth Mountains of central Idaho. With these analyses, we address the following questions:

1. How do unique watershed structures and stream network geometries lead to spatially variable patterns of hydrologic turnover in synthetic and natural watersheds that manifest as variable stream source compositions?

2. What are the implications of network scale hydrologic turnover for interpreting stream network signals?

2. Methods

We performed conservative tracer (chloride, Cl^-) injections on 10 stream reaches within the Bull Trout watershed in the Sawtooth Mountains of central Idaho to quantify net changes in Q and gross hydrologic exchanges between stream water and groundwater along each reach. Empirical relationships derived from these experiments became the basis of a network model that simulates hydrologic gains, losses, and turnover along stream networks.

2.1. Study Area

We selected six watersheds located within 70 km of one another in the Sawtooth National Forest of central Idaho for this study. Watersheds range in size from 11.4 to 64.0 km^2 and in elevation from 1957 to 3256 m (Figure 1). Thirty-year average annual precipitation is 108 cm, with 64% occurring as snowfall (Banner Summit snowpack telemetry, SNOTEL, 312, 2146 m elevation, located within 55 km of all watersheds). Land cover on hillslopes and at higher elevations is dominated by lodgepole pine (*Pinus contorta*) in the subalpine zone and grasses in the alpine zone; land cover in the valley bottoms is a mix of lodgepole pine (*Pinus contorta*), sedges (*Carex* spp.), grasses, and willows (*Salix* spp.). Parent lithology is biotite granodiorite of the Idaho Batholith, and valley fill is composed of Pleistocene till mixed with Holocene alluvium and colluvium [*Kiilsgaard et al*., 2003].

2.2. Field Hydrologic Measurements

Hydrologic data were collected in all watersheds to quantify annual, seasonal, and hourly discharge. We additionally measured streamwater-groundwater exchange across a broad range of watershed positions

and flow states in Bull Trout watershed. Field experiments were performed from May to September during 2006 and 2007. Measurements included salt dilution gauging [*Covino et al*., 2011; *Kilpatrick and Cobb*, 1985], tracer mass recovery experiments [*Covino et al*., 2011; *Covino and McGlynn*, 2007; *Payn et al*., 2009], and discharge measurements via continuous stage measurement and rating curves.

Stream discharge was computed at the outlets of each watershed using continuous stage measurements (capacitance rods; TruTrack, Inc.; vertical resolution of 1 mm and temporal resolution of 10 min–1 h). Rating curves for each watershed outlet were calculated using periodic discharge measurements (velocity-area method and salt dilution gauging). Discharge was additionally measured at spatially distributed locations within Bull Trout using salt dilution gauging methods.

We performed conservative tracer mass recovery experiments [see *Covino et al*., 2011 for detailed methods] in 10 separate reaches (191–3744 m) that spanned the range of flow states ($\sim$1–800 L s^{-1}) and stream types (first-order headwater to third-order valley bottom stream) for a total of 16 tracer experiments in Bull Trout watershed to quantify changes in discharge across a reach as well as gross gains and losses of stream water to and from groundwater. Short distance slug additions of sodium chloride (NaCl) were injected first at the base and then at the head of each reach and used to determine local discharge at each of those locations via salt dilution gauging [*Covino et al*., 2011; *Kilpatrick and Cobb*, 1985]. The difference between these two discharge measurements equals the net change in discharge (ΔQ_{NET}) along that reach; ΔQ_{NET} is negative if the downstream discharge measurement is lower than the upstream, and vice versa. We selected injection locations and reach lengths to ensure full mixing of added tracer and confirmed this mixing with visual observation of rhodamine dye injections. Additionally, we quantified the mass of chloride (Cl^-) injected at the head of the reach that was recovered at the base of the reach. From the mass injected at the head of the reach, we were able to calculate the percent mass of chloride lost. This calculated percent mass lost was equated to the gross percentage of discharge lost; gross loss of discharge (Q_{LOSS}) is the product of percent loss and local discharge at the head of the reach. The decision to use the discharge at the head of the reach rather than base was made as a more conservative estimate of loss. Although a negative Q_{LOSS} is mathematically possible in the event that more tracer was recovered than injected, this scenario is practically impossible and was never observed here or in previous studies using the same method [*Covino et al*., 2011; *Payn et al*., 2009]. Gross gain of discharge (Q_{GAIN}) is calculated using mass balance:

$$Q_{GAIN} = \Delta Q_{NET} + Q_{LOSS} \tag{1}$$

where again, over a given reach ΔQ_{NET} is the net change in discharge. We therefore quantified reach scale tracer dynamics and corresponding water balances using direct, experimental methods.

2.3. Terrain Analysis

We performed terrain analysis using digital elevation models (DEMs) derived from airborne laser swath mapping (ALSM) and USGS quadrangle maps. These DEMs were supplemented with GPS-surveyed streamlines, which were collected in four of the six watersheds (Bull Trout, Pettit, Stanley, and Alturas). Watersheds were surveyed using a Trimble GeoXT GPS and differentially corrected using the Payette National Forest base station in McCall, ID ($\sim$120 km away). ALSM data were collected on 2 September 2009 by the National Center for Airborne Laser Mapping (NCALM). Instrument vertical and horizontal accuracy was 5–30 and 10 cm, respectively. Point cloud data were filtered to a bare earth DEM with a resolution of 1 m and resampled to 10 m for this analysis to correspond to USGS DEMs. USGS quadrangles of 10 m resolution were downloaded from the USGS seamless server: data available from the USGS, Earth Resources Observation and Science (EROS) Center, Sioux Falls, SD.

Prior to delineating watershed boundaries, we applied a drainage-route deepening algorithm [*Olaya*, 2004] to each DEM to eliminate sinks in the relatively flat valley-bottoms. We chose to deepen drainage routes rather than fill sinks due to the loss of valley-bottom topography caused by sink-filling algorithms in these watersheds. After deepening drainage routes, we delineated the boundaries of each watershed using a single flow direction algorithm (D8) [*O'Callaghan and Mark*, 1984].

Upslope accumulated area (UAA) at each watershed cell was calculated using a triangular multiple flow-direction algorithm (MD∞) [*Seibert and McGlynn*, 2007] up to the field observation corroborated stream

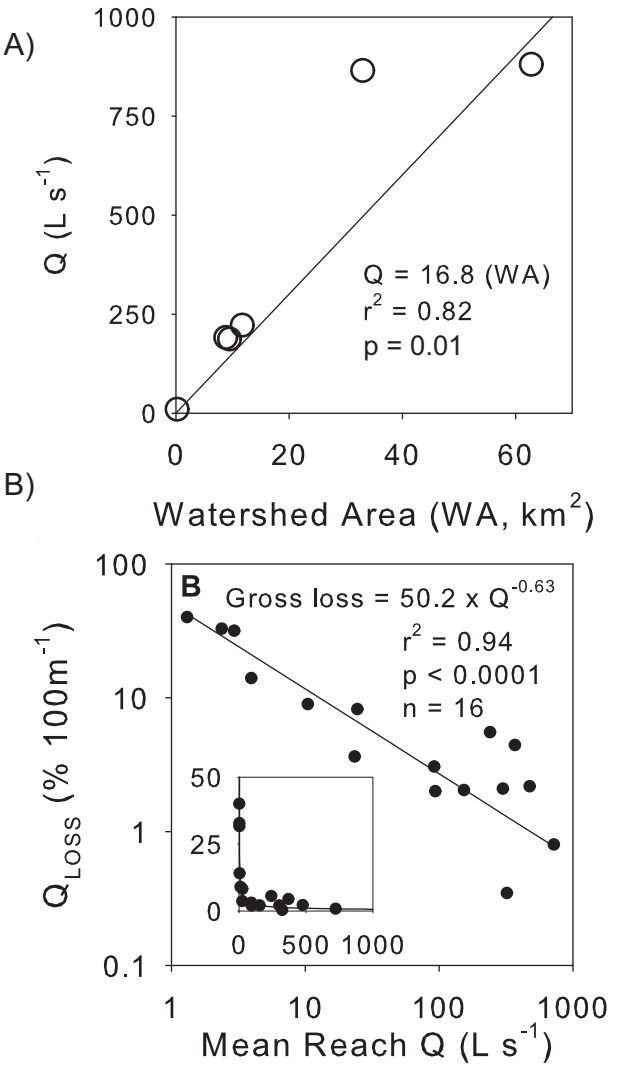

Figure 2. Empirical relationships between (a) watershed area and discharge across all six watersheds with linear regression; and (b) discharge and % loss of discharge per 100 m of channel length with negative power law regression (modified from *Covino et al.* [2011]).

channel initiation threshold of 20 ha, after which area was routed downstream using a single-direction flow algorithm (D8). Watershed cells downstream of cells where a channel was initiated were classified as stream cells. For these stream cells (i.e., 10 m stream reaches), we also calculated total watershed area and local input (LI) [*Grabs et al.*, 2010; *Jencso et al.*, 2009; *McGlynn and Seibert*, 2003]. LI is the area that contributes water directly to a given reach and does not include area that contributes water indirectly through upstream reaches (often alternatively described as a lateral inflow).

Stream networks generated from this process were visually checked against the GPS streamlines, the 1 m ALSM DEM and Digital Ortho Quarter Quads (digital aerial images) for agreement with observed stream networks. Minor, manual terrain modifications were made in some cases based on these auxiliary data to correct unrealistic or unobserved flow paths along each stream network.

We used the outputs from these terrain analyses (stream networks, local inputs to those stream networks, and watershed area for each stream cell calculated from upstream accumulated local inputs) as scaling factors to extend our measured hydrologic variables (Q_{GAIN}, Q_{LOSS}, and ΔQ_{NET}) from the reach scale at which they were measured to the stream network scale in all six natural and seven synthetic watersheds using the following empirical relationships.

2.4. Empirical Relationships

We quantified two empirical relationships between our measured hydrologic variables (Q_{GAIN}, Q_{LOSS}, and ΔQ_{NET}) and observed watershed terrain metrics (Figure 2). First, we quantified the relationship between area and discharge:

$$\Delta Q_{NET,i} = \alpha^* LI_i \tag{2}$$

where $\Delta Q_{NET,i}$ is net discharge gained across a reach, i; LI_i is the local input at reach i. Because the Q–A relationship (Figure 2a, equation (2)) is specific to a given day, our model is at steady state for that given day, and we assume that the system is in hydrologic equilibrium. Second, we quantified the relationship between discharge and percent loss of discharge:

$$\%Loss_i = \beta Q_{i-1}^{\gamma} \tag{3}$$

where $\%Loss_i$ is the percent of discharge lost to groundwater in reach i; α, β, and γ are regression parameters fit to linear (α, equation (2)) and power law (β and γ, equation (3)) forms; and Q_i is the mean discharge

through reach *i*. Regression parameters α and β have units of length per time and time per volume, respectively. The parameter γ is unitless. Since the regression shown in Figure 2b is scaled to losses over 100 m but the DEM is 10 m resolution, we downscaled the percent loss by a factor of 10.

The relationship between discharge and area (Figure 2a, equation (2)) is based on six measurements of discharge collected at six locations across three watersheds on 24 July 2006. We use a single day's worth of measurements because the relationship between discharge and area varies with the hydrograph. Five of these measurements were based on stage measurements and rating curves at five locations in Stanley, Alturas, and Bull Trout watersheds. The sixth was taken using salt dilution gauging in the headwaters of Bull Trout watershed. These discharge measurement locations spanned a broad range of watershed area amongst all six watersheds (<1 km^2 to the largest at 64 km^2). Based on the assumption that our measurements apply across the watersheds, we leveraged these two relationships (equations (2) and (3)) in conjunction with our terrain analysis to extend our field measurements to the stream network scale.

2.5. Synthetic Watersheds

We generated seven synthetic watersheds for comparison against the six natural watersheds to elucidate how hydrologic turnover can propagate through radically simplified watersheds and stream networks, and to provide context for interpretation of our results from the more complex, natural watersheds. The total watershed areas and network lengths of these synthetic watersheds were selected to lie within the range observed in the natural Sawtooth watersheds. Three of these networks varied in their stream network geometry while four varied in their watershed structure (the organization of convergent and divergent hillslopes). The networks that varied in network geometry ranged from 0 to 2 levels of network bifurcation (Table 1). Those networks that varied in watershed structure varied in two ways: the shape of the distribution of local inputs and their organization (i.e., either skewed toward headwaters or toward the outlet; Table 1). Two watersheds had area distributed with a binary distribution and two with a gamma distribution. Each distribution was parameterized by the actual frequency distribution of LI in the six Sawtooth watersheds. Two of these watersheds (one binary and one gamma) were sorted with the highest LI in the headwaters and two were sorted with the highest LI closest to the watershed outlet (Table 1).

2.6. Conceptual Model of Stream Gains, Losses, and Hydrologic Turnover

In our conceptual model (Figure 3), water enters a stream reach either from an upstream reach or a lateral input from groundwater. Once in the reach, water from all sources is assumed to be fully mixed and therefore proportionally subject to loss from the stream reach to groundwater. The result of these simultaneous gains and losses, when propagated longitudinally through the network, is hydrologic turnover. The output from each reach, then, is a constantly shifting mixture of water from all upstream sources (Figure 3a). If overall discharge magnitude is tracked moving in the downstream direction and separated into its source components, it is evident that even as discharge increases due to increasing inputs of area, both the absolute and relative magnitudes of contribution from upstream sources diminish due to compounding hydrologic turnover (Figure 3b).

2.7. Implementation of Conceptual Model

We implemented our analytical framework that utilized the empirical relationships described above (equations (2) and (3)) in conjunction with terrain analysis to extend the hydrologic variables measured at the reach scale (Q_{GAIN}, Q_{LOSS}, and ΔQ_{NET}) along the stream networks in each of the six watersheds. The water balance equation for each stream reach is a slight modification of equation (1):

$$Q_i = Q_{i-1} + Q_{i,GAIN} - Q_{i,LOSS} \tag{4}$$

where Q_i is the discharge in a reach, *i*, and Q_{i-1} is the discharge in the reach(s) immediately upstream. $Q_{i,GAIN}$ and $Q_{i,LOSS}$ are the gain and loss to and from reach *i* and are calculated using the water balance and empirical relationships previously described (equations (1–3)). $Q_{i,LOSS}$ can be calculated as the product of discharge entering reach *i* and the percent loss in that reach (i.e., $\%Loss_i$ from equation (3)). Equation (4) is

Table 1. Basic Watershed Characteristics for All Six Natural and All Seven Synthetic Watersheds Analyzed in This Study Including *Horton*'s [1932] Form Factor[a]

Watershed	Map	Main Stem Length (km)	Watershed Area (km^2)	Horton's Form Factor (Area/Length^2)	$Q_{1/2}$
Bull Trout		6.6	11	0.25	0.34
Hellroaring		12.3	15	0.10	0.23
Pettit		10.3	23	0.22	0.38
Yellowbelly		15.2	28	0.12	0.28
Stanley		13.5	33	0.18	0.31
Alturas		14.6	64	0.30	0.42
One bifurcation		14	15	0.08	0.20
Two bifurcations		11	15	0.12	0.30
Three bifurcations		7	15	0.31	0.42
Binary—high to low		14	11	0.06	0.22
Binary—low to high		14	11	0.06	0.15
Gamma—high to low		14	11	0.06	0.27
Gamma—low to high		14	11	0.06	0.07

[a]$Q_{1/2}$ is the proportion of the stream network closest to the outlet that contributes $^1/_2$ of the discharge at the outlet.

solved iteratively starting in the headwaters (where Q_{i-1} is set to zero as a boundary condition) and moving in a downstream direction along the stream network.

In order to determine sourcewater mixtures at reach *i*, we calculated a stream water turnover factor, TF, as a measure of the proportion of stream water gained from groundwater in reach *i* relative to the discharge input from the upstream reach and the discharge lost from reach *i*.

$$TF_i = 1 - \frac{Q_{i,GAIN}}{Q_{i-1} - Q_{i,LOSS} + Q_{i,GAIN}} \tag{5}$$

This turnover factor is the proportional contribution to Q_i from all upstream reaches and can be conceptualized as the influence that a given input has on the composition of stream water. The *TF* is bounded between 1 and 0. $Q_{i,GAIN}$ is positive because area increases in the downstream direction (equation (2)). The denominator

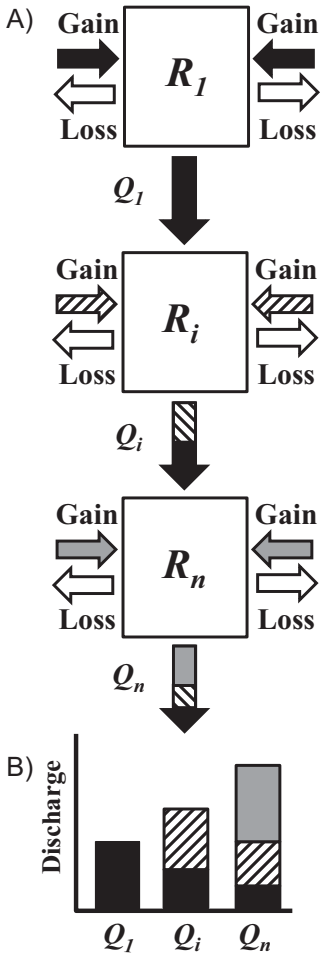

Figure 3. (a) Conceptual model of simultaneous gross gains and losses, hydrologic turnover, and shifting source compositions of discharge output from each reach. (b) Discharge output from each reach with height of overall and individual bars corresponding to total discharge and discharge contribution from each specific reach, respectively.

of this relationship is always positive because the loss is calculated as a percentage of stream discharge and measured discharge is never low enough to result in 100% or greater loss (Figure 2). Therefore, the *TF* is always greater than zero. $Q_{i,GAIN}$ occurs in both the numerator and denominator, implying that *TF* must always be less than one. An increase in either $Q_{i,GAIN}$ or $Q_{i,LOSS}$ increases the right hand term in equation (5), and therefore decreases the *TF*. Conceptually, a lower turnover factor means there is less water remaining in reach *i* from upstream reaches relative to the gain in reach *i*.

We used *TF* to calculate the discharge added to the stream in reach *i* ($Q_{i,GAIN}$) that remains in the reach immediately downstream, $i + 1$:

$$Q_{i+1,i} = Q_{i,GAIN} * TF_{i+1} \quad (6)$$

where $Q_{i+1,i}$ is the amount of discharge remaining in reach $i + 1$ from reach *i*. This equation can be generalized to calculate the contribution from any upstream reach, *j*, by recognizing that its turnover factor, TF_j, is the product of all TF_i between reach *j* and reach $i - 1$:

$$Q_{i,j} = Q_{j,GAIN} * \prod_{k=j}^{i-1} TF_k \quad (7)$$

The distribution of $Q_{i,j}$ across all *j* is the distribution of all distinct spatial inputs to reach *i*.

Equation (7) well illustrates hydrologic turnover $\left(\prod_{k=j}^{i-1} TF_k\right)$. It is quantified by the product of successive TFs between two flow-connected points within the stream network; therefore, it is a unitless measure of the magnitude of stream-groundwater interactions through a stream network.

3. Results

3.1. Empirical Relationships

We applied measured reach scale streamwater-groundwater exchange across the network using two empirical relationships. The linear relationship between watershed area and *Q* (Figure 2a) was derived from discharge measurements in Bull Trout, Stanley, and Alturas watersheds that span the range of watershed areas (<1–64 km^2) and flow states (<10–900 L s^{-1}). The relationship is well characterized with a linear fit ($R^2 = 0.82$, $p = 0.01$, Figure 2a). Tracer mass recovery experiments were performed to determine reach water balance components across a range of flow states and spatial locations in Bull Trout watershed. These experiments revealed a negative power law relationship between *Q* and % loss of *Q* per 100 m of stream ($R^2 = 0.94$, Figure 2b). Loss ranged between ~40% at flows of 2 L s^{-1} and <1% at flows approaching 900 L s^{-1}. These empirical relationships were used to extend our reach-scale measurements across multiple stream networks within the framework of our conceptual model (Figure 3).

3.2. Hydrologic Turnover at the Stream Network Scale

3.2.1. Shifting Mixtures of Stream Source Compositions

We implemented our conceptual model (Figure 3) in two ways across the entire Bull Trout watershed (Figure 4): without hydrologic turnover (Figure 4a) and with hydrologic turnover as described mathematically in

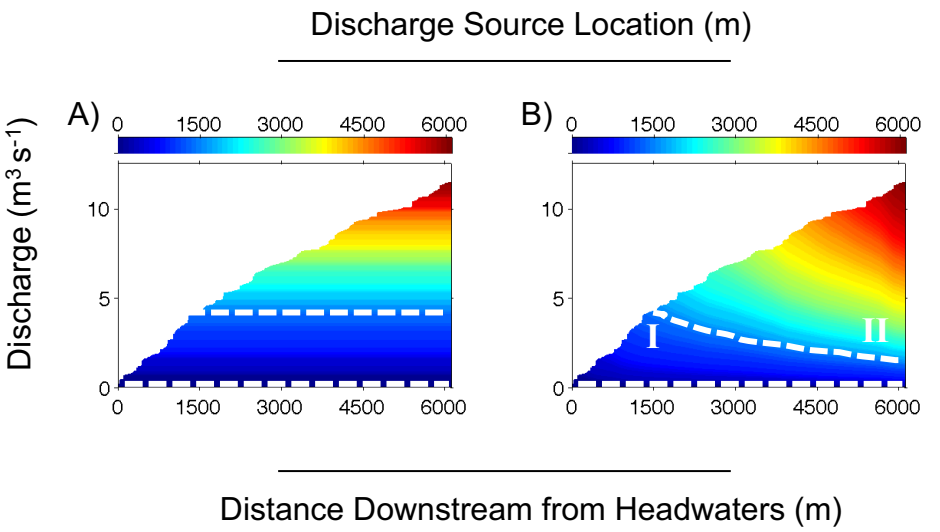

Figure 4. Overall discharge magnitude and source composition moving downstream in Bull Trout watershed with (a) no hydrologic turnover and (b) showing the effects of hydrologic turnover. The overall height of the trend at any distance corresponds to the total discharge at that distance downstream from the headwaters. The vertical thickness of each color band represents the magnitude of the contribution to total discharge from the corresponding distance on the color bar at the top of each plot as it evolves through the stream network. Note the change in thickness of the blue color band (water from headwater locations) moving from (I) to (II) as indicated by the dotted line in Figure 4b contrasted to the lack of change in Figure 4a. This narrowing in Figure 4b indicates that water from the headwaters has been lost en route to the outlet due to hydrologic turnover, contrasted with Figure 4a in which no loss has occurred in the absence of hydrologic turnover.

section 2.7 (Figure 4b). Total network discharge is represented by the height of the plot at each network distance. The thickness of a color band at any given network distance is the absolute magnitude of discharge contribution from the corresponding distance downstream from the headwaters on the color bar above each plot. The absence of turnover is illustrated by the horizontal stratification of each color band, and specifically highlighted by the white dotted line (Figure 4a). These patterns indicate that in the absence of hydrologic turnover, the amount of input from each network location stayed constant as it was transported downstream, regardless of distance. Results from Bull Trout that include hydrologic turnover (Figure 4b) display similar shifts in source water mixtures as our conceptual model (Figure 3b), with the relative and absolute contribution of a given input to the stream network diminished moving downstream through the stream network. This deterioration of each source's contribution due to hydrologic turnover is visibly evident (Figure 4b) as a pinching or narrowing of each color band moving downstream from the headwaters (left) to the outlet (right). This effect of turnover is highlighted by the white, dotted lines outlining the blue (headwater) color band.

At a given network distance, steeper positive slopes in overall discharge accumulation or steeper negative slopes between color bands represent a higher degree of hydrologic turnover due to either greater gains or losses at that location, respectively. The result of this reduction of each hydrologic input moving downstream is that the mixture of source waters at the outlet of the watershed is strongly skewed toward more proximal (red/orange) locations than more distant (blue), headwater locations. Therefore, in contrast to results in the absence of hydrologic turnover (Figure 4a), the mixture of source waters at downstream locations is not evenly reflective of the comparative magnitudes of inputs from proximal and distant locations (Figure 4b).

3.2.2. Synthetic Watersheds

Three of the synthetic watersheds varied in their network geometries (Table 1 and Figure 5), with two, one, or no levels of bifurcation in their networks. The remaining four varied in their upland shapes, resulting in spatial distributions of local inputs (LI) that either increased or decreased from the headwaters to the outlet, and did so with either a binary distribution of LI or a gamma distribution of LI following the sorted frequency distribution of LI in the actual Sawtooth watersheds (Table 1 and Figure 6).

Shifts in source water mixtures due to hydrologic turnover followed the same general pattern as our conceptual model (Figure 3): the relative and absolute contribution of a given input diminished moving downstream through the stream network as illustrated by a pinching of each color band moving from the

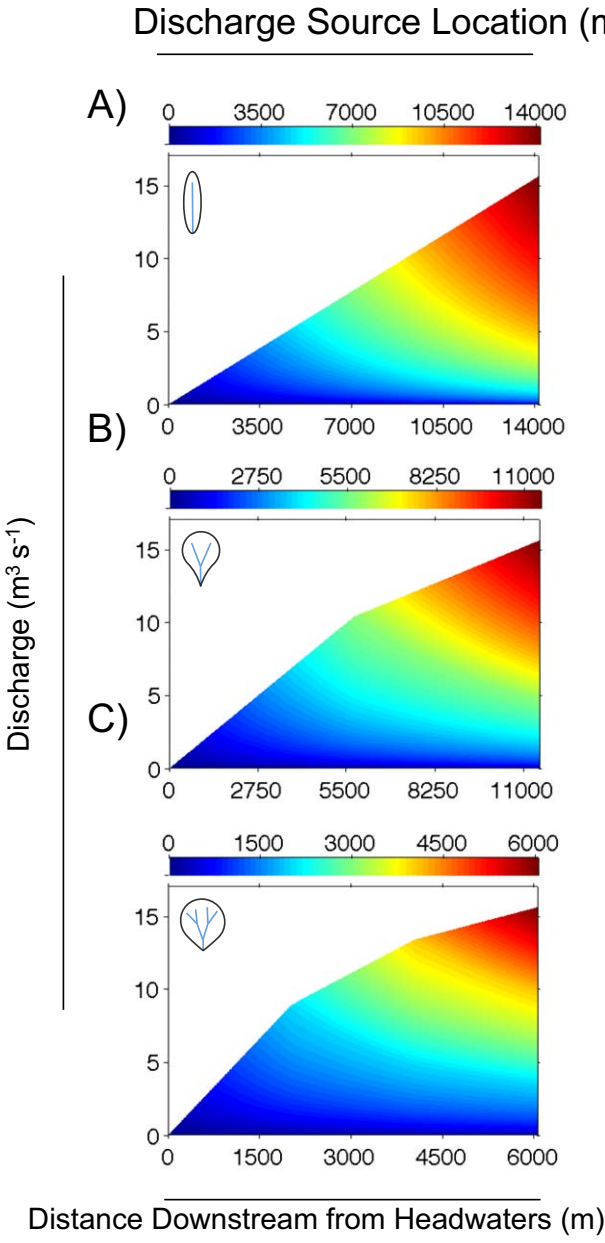

Figure 5. Overall discharge magnitude and shifting source compositions moving downstream in three synthetic watersheds with (a) no, (b) one, and (c) two levels of bifurcation. The overall height of the trend at any distance corresponds to the total discharge at that distance downstream from the headwaters. The vertical thickness of each color band represents the magnitude of the contribution to total discharge from the corresponding distance on the color bar at the top of each plot as it evolves through the stream network.

headwaters to the watershed outlet (Figure 5). Therefore, the mixture of source waters at downstream locations is not evenly reflective of the initial magnitudes of inputs from across the stream network (Figure 5).

Moving along a gradient from no network bifurcation to two levels of bifurcation (Figure 5), it is evident that even with the same total stream network length, changing network geometry results in shifting source mixtures. Although the ultimate discharge magnitude in each network is the same, the discharge accumulates increasingly in the headwaters with more bifurcations as evidenced by the increasing convexity of the overall discharge accumulation from Figures 5a–5c.

This increasing influence of the headwaters with successive bifurcations is also evidenced in both the peak magnitude and final magnitude of the blue color band, which represents sources of local inputs farthest from the outlet (Figures 5a–5c). The most bifurcated network (Figure 5c) had a higher accumulation of discharge in locations farther from the outlet, and also a higher proportion of its final discharge from these locations. This network received 30% of its discharge at the outlet from these headwater sites, compared to 17% and 7% for the networks with one and no bifurcations, respectively (Figure 5). Another way to characterize the variability in source water compositions is the proportion of the network nearest to the outlet that contributes half the magnitude of outlet Q ($Q_{1/2}$). In these synthetic watersheds, $Q_{1/2}$ varies (Table 1) from the lower 0.2 of the network (Figure 5a) to 0.42 in the twice-bifurcated network (Figure 5c). A low $Q_{1/2}$ indicates that more of the outlet discharge is contributed by closer locations, and a smaller proportion of the network that lies near the outlet more heavily influences outlet signatures.

Similar results to those described above are evident in synthetic watersheds whose network geometries remain constant as a nonbifurcated channel, but whose watershed shapes vary. While these watersheds all have the same area, the spatial distribution of that area varies (Figure 6 and Table 1). The discharge accumulation pattern in watersheds in which area is distributed with the majority in the headwaters is convex (Figures 6b and 6d) similar to the bifurcated networks mentioned previously (Figures 5b and 5c). In contrast, the watersheds with more area accumulated toward the outlet manifest this distribution as a concave discharge accumulation (Figures 6a and 6c).

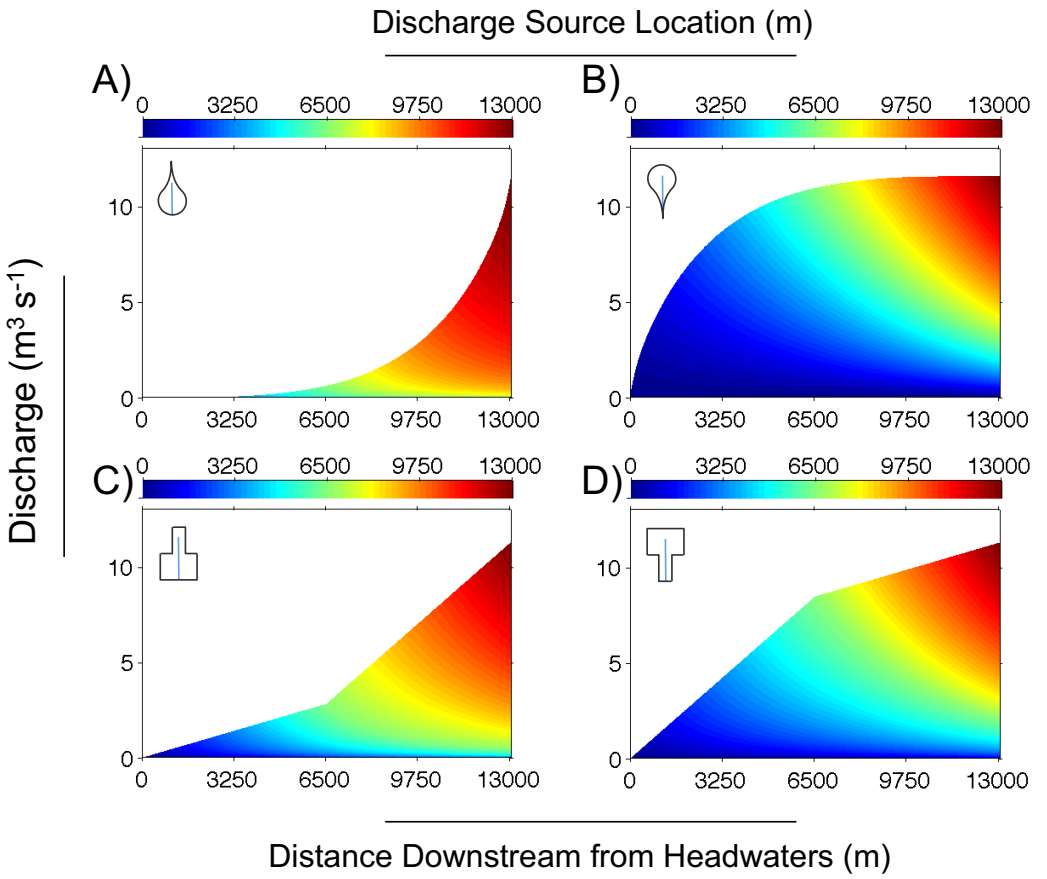

Figure 6. Overall discharge magnitude and shifting source compositions moving downstream in four synthetic watersheds with varying distributions of local inputs to stream networks. The overall height of the trend at any distance corresponds to the total discharge at that distance downstream from the headwaters. The vertical thickness of each color band represents the magnitude of the contribution to total discharge from the corresponding distance on the color bar at the top of each plot as it evolves through the stream network. Local inputs are distributed using either a gamma distribution fit to actual Sawtooth Mountain (a and b) local input distributions or (c and d) a binary distribution. Distributions are sorted either from small inputs in the headwaters to large inputs toward (a and c) the outlet or (b and d) the reverse.

Figures 6a and 6b represent extreme examples of sorted LI, with one receiving the majority of its area inputs near the outlet (Figure 6a) and the second receiving the most inputs in the headwaters (Figure 6b). This results in distinct mixtures of source waters at the outlet of each watershed. $Q_{1/2}$ at the watershed outlets of these four watersheds varies (Table 1) from 0.7 (Figure 6a) to 0.27 (Figure 6b). Although all watersheds exhibit diminishment in contribution from headwater locations to their outlet source compositions, higher accumulation in headwaters induces relative stability in source compositions. For example, the diminishment of discharge from headwater sources (i.e., the decrease in the thickness of the blue color band) is much smaller (within an order of magnitude) in Figure 6d than Figure 6c (a change of more than an order of magnitude).

Despite these differences, hydrologic turnover exerts a common influence on all of these watersheds: by way of example, although 75% of the area in watershed in Figure 6b is accumulated in the headwaters, these locations (blue in Figure 6b) contribute only ~10% of total discharge at the outlet due to compounded hydrologic turnover through the stream network. Likewise, the headwaters of the most bifurcated watershed (Figure 5c) contributed ~35% of the area but accounted for only ~13% of the stream source composition at the outlet.

3.2.3. Natural Watersheds

Model results from the six Sawtooth watersheds display patterns broadly reminiscent of the synthetic watersheds described above but with greater complexity due to their more complex shapes (Figure 7). Overall discharge accumulates steadily in each watershed moving downstream, but with rates of

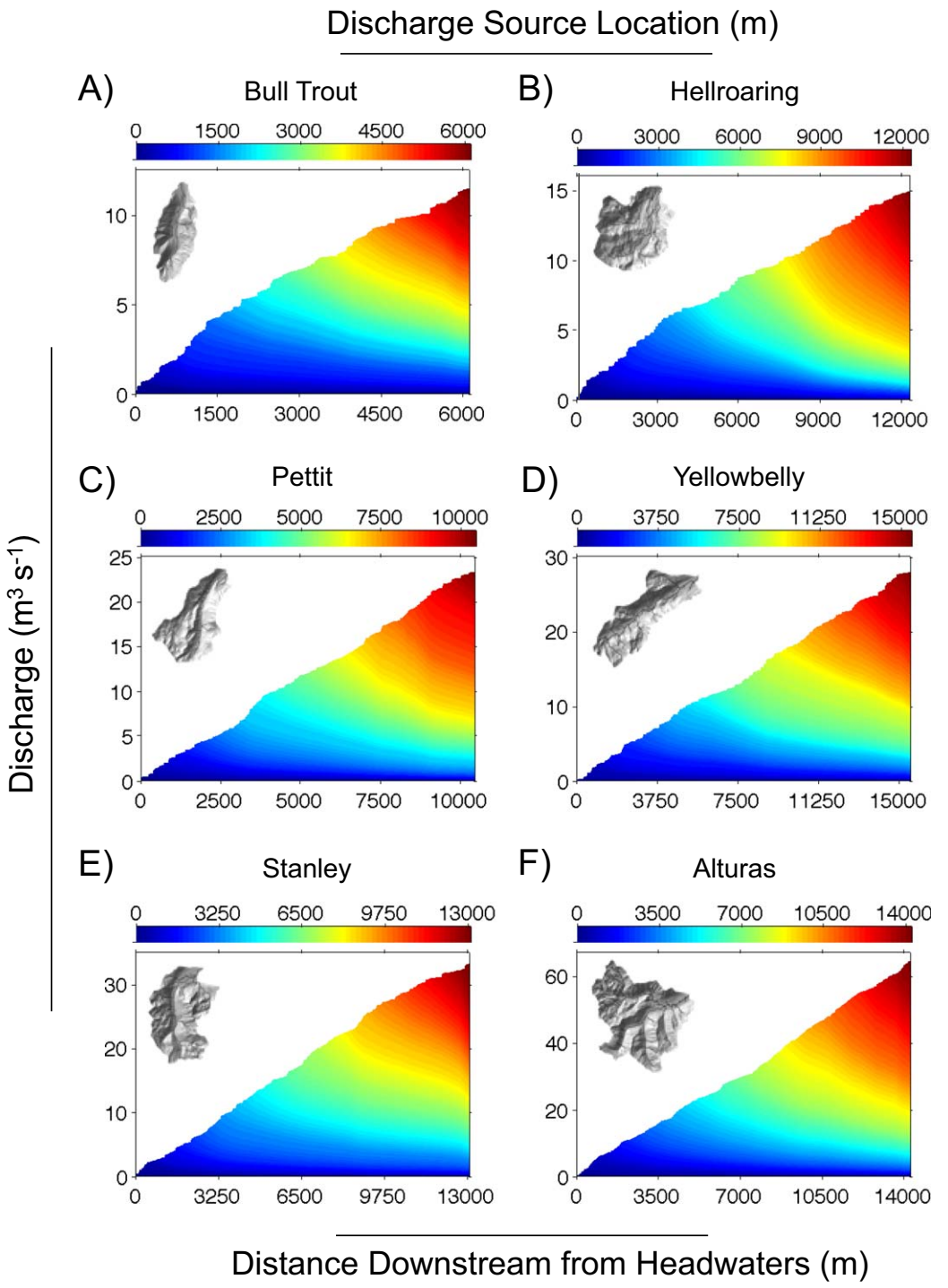

Figure 7. Overall discharge magnitude and shifting source compositions moving downstream through each of the six watersheds. The overall height of the trend at any distance corresponds to the total discharge at that distance downstream from the headwaters. The vertical thickness of each color band represents the magnitude of the contribution to total discharge from the corresponding distance on the color bar at the top of each plot as it evolves through the stream network. Watersheds are arranged from the (a) smallest to (f) largest watershed areas.

accumulation varying based on the distribution of watershed LI along each stream network. These variable rates of area and *Q* accumulation are visibly evident as small convexities and concavities inset in the overall increasing trend in *Q* (Figure 7). The contributions of each spatial source of stream water decay as they move downstream toward the outlet due to hydrologic turnover as illustrated in our conceptual model (Figure 3).

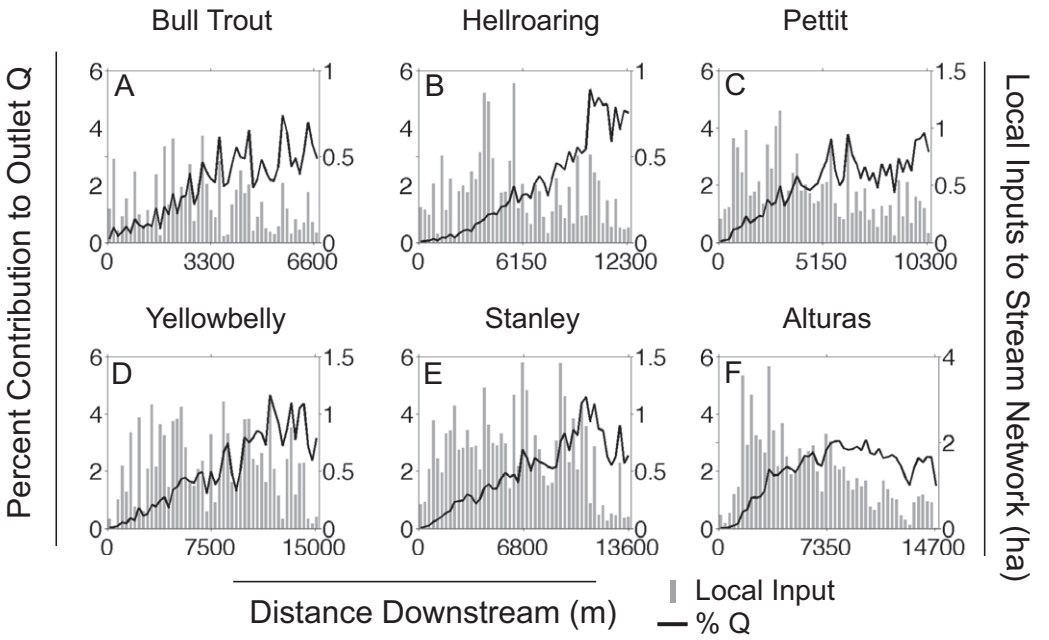

Figure 8. Distribution of local inputs with distance downstream from headwaters for each watershed (gray bars) with headwaters at zero and outlet at far right of each plot. Overlain on distribution of percent contribution to discharge at outlet from each network distance (black lines). Magnitudes of both bars and lines are summed magnitudes across all network positions that share the same distance class.

However, because each watershed has a unique distribution of LI and stream network geometry, the distinct patterns in the pinching and slope of the color bands in each plot (Figure 7) changes from watershed to watershed. At a given network distance, steeper positive slopes in overall discharge accumulation or steeper negative slopes between color bands represent a higher degree of hydrologic turnover due to either greater gains or losses at that location, respectively. $Q_{1/2}$ in these watersheds varies from a low of 0.23 in Hellroaring to a high of 0.42 in Alturas (Table 1). Because the ordering of each watershed by $Q_{1/2}$ reveals no general trend based on, for example, overall watershed area or network length, variability in $Q_{1/2}$ amongst the natural watersheds cannot be completely explained by general watershed characteristics like network length or watershed size (Table 1).

A vertical slice through each plot in Figure 7 at each watershed outlet (right side of each plot) is the distribution of absolute contributions to discharge from each upstream location. When these distributions are normalized to total discharge in each watershed (Figure 8, black lines) they can be compared across watersheds as percent contribution to discharge. The corresponding distributions of LI at each upstream location (Figure 8, gray bars) represent the spatial inputs of water to the network at a given distance. When compared in this way it is evident that sections of the network with large local inputs correspond in location along the *x* axis to peaks in relative contribution to the outlet from those locations, but they become increasingly decoupled in magnitude as we move further away from the outlet (further to the left on the *x* axis). In contrast, the distributions of contributions to discharge for each of the upstream locations (Figure 8, black lines) reveal a trend in five of the watersheds (Figures 8a–8e) of increasing contribution with proximity to the outlet, an observation similar to that exhibited in Figures 4–7. The distribution of contribution to discharge in Alturas increases initially but starts to flatten and even decreases at ~7000 m downstream from the headwaters (Figure 8f). Although this runs counter to the trend observed in the other watersheds, it can be partially accounted for by observing that the downward trend in the distribution of LI moving toward the outlet is much steeper in Alturas than in the other watersheds (Figure 8f). This interpretation can be supported by consideration of Figures 5c and 6b. Although highly convoluted by hydrologic turnover, the initial structure of the input (in this case, dramatically higher inputs in the headwaters) is still evident in the final source composition.

The cumulative distribution of percent contribution to discharge (Figure 9) illustrates the different distance scales that contribute discharge to the outlet of watersheds. Percent contribution to discharge shown here

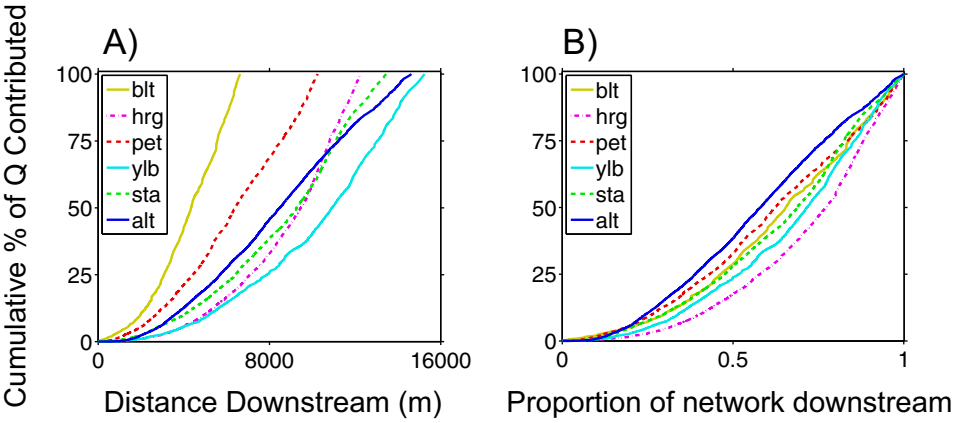

Figure 9. Cumulative spatial distributions of percent contribution to discharge at the watershed outlet moving downstream through each stream network: Bull Trout (blt), Hellroaring (hrg), Pettit (pet), Yellowbelly (ylb), Stanley (sta), and Alturas (alt). Discharge accumulated along the network in either (a) actual distance downstream from furthest headwater or (b) network distance normalized to the length of each network. Steeper slopes correspond to more accumulation of discharge at that location in the network.

is the same shown in Figure 8, though presented here as a cumulative rather than frequency distribution. The local slope of each distribution corresponds to the magnitude of contribution from that distance, with steeper slopes indicating higher contributions from those locations. Therefore, each watershed displays a general trend of increasing slope moving downstream (from left to right). The relative sorting of the watersheds changes moving through from headwaters (at 0%) to outlet (at 100%). At 50% of discharge contribution, the order of Alturas, Stanley, and Hellroaring is reversed from the order at 100% discharge (Figure 9a). The distance at which each watershed's distribution crosses the 50th percentile is the distance that divides the network into two portions that each contribute half of the discharge at the outlet. The size of the downstream portion relative to the overall network corresponds to the $Q_{1/2}$ (Figure 9b and Table 1). This downstream portion is shorter than the upstream portion in each watershed due to hydrologic turnover weighting the parts of the network closer to the outlet more heavily.

4. Discussion

As introduced preliminarily in *Covino et al.* [2011], our results illustrate the connection between hydrologic turnover (the simultaneous or sequential loss and gain of water to and from groundwater, propagated longitudinally through a stream network) and the ultimate source water composition of stream water at the watershed outlet. The source composition at a watershed outlet is a representation of the relative and absolute magnitudes of contributions of water and associated solutes from each distance upstream of the outlet to that source composition. We emphasize that by "source" we refer to the most recent location that water enters the channel from groundwater within our modeling framework. Our analysis demonstrates that hydrologic turnover at the stream network scale can strongly modify stream water source composition as illustrated in both synthetic and natural watersheds. Hydrologic turnover modifies source compositions in two ways: by diminishing the magnitude of spatial inputs to the stream network through losses to groundwater and by further diluting all inputs with gains from groundwater. Here we expand our analysis beyond a single watershed to elucidate connections between variable watershed morphologies and outlet source compositions.

4.1. How Do Unique Watershed Structures and Stream Network Geometries Lead to Spatially Variable Patterns of Hydrologic Turnover in Synthetic and Natural Watersheds That Manifest in Variable Stream Source Compositions?

We expand the analysis presented in *Covino et al.* [2011] by incorporating a spectrum of watershed structures and stream network geometries into the analytical framework presented therein and expanded upon here. The results presented here are derived from seven synthetic and six natural watersheds. By extending our analysis beyond the initial study watershed, we can directly address how spatial patterns of hydrologic

turnover vary between watersheds and additionally how this variability can control the unique evolution of source composition in a range of watersheds.

The spatial distributions of hydrologic turnover are set by the magnitudes of discharge gained from and lost to groundwater along the stream network. Since gross hydrologic gains and losses vary spatially in conjunction with watershed LI and stream discharge, respectively, and because each watershed has unique network geometry, the spatial pattern of hydrologic turnover is specific to each watershed. The patterns in the color bands of Figures 4–7 illustrate how source compositions vary with distinct patterns in synthetic and natural watersheds due to the "finger prints" of each watershed.

4.1.1. Synthetic Watersheds

The synthetic watersheds presented here, by virtue of their basic shapes, facilitate interpretation of our results. As end-members on spectrums of watershed structure and network geometry and additionally as basic building blocks of natural watersheds, they can be used to bracket or interpret expected results in natural watersheds. The synthetic watersheds exhibit variability in their source compositions due to distinct accumulations of area or geometries in each, and this variability can be directly related to simple differences in either geometry or watershed structure between them. Watersheds that accumulate area predominately in their headwaters (upper 1/3 of the stream network, blue on color ramp; Figures 5b, 5c, 6b, and 6d) show source compositions with a greater contribution from those further locations than nonbifurcated watersheds or those that accumulate more area closer to the outlet (Figures 5a, 6a, and 6c). Although this general observation is intuitive, it is important to realize that the actual magnitude of the contribution from headwater locations in these watersheds is strongly modified (i.e., diminished) by hydrologic turnover moving through the network.

Stream network geometry and watershed structure can have similar effects on the evolution of source composition, though there are some important distinctions. Increasing bifurcation can induce source water compositions similar to that of watersheds that are increasingly bulbous in their headwaters: discharge increases with a convex rather than concave shape moving downstream and the source composition is weighted less heavily toward proximal outlet locations (e.g., see Figures 5c and 6c for general comparison). In both of these cases, more water from headwater sources remains part of the source composition at the outlet due to greater inputs, although still less than the initial magnitudes of those inputs. It is here where a distinction between these two examples arises. Because fractional discharge lost is smaller in reaches with higher discharge, concentrated gains in the headwaters induce some stability in the contribution of these headwater locations. In contrast, bifurcation can have the opposite effect on turnover: it can separate local inputs to the stream network, and therefore discharge into smaller inputs resulting in higher percent losses in each reach (Figures 2b and 5).

The radically simplified shapes of these watersheds, though physically unrealistic, are valuable in facilitating interpretation of the more complex shapes observed in the natural watersheds (Figure 7). Convexity versus concavity of the patterns of discharge accumulation (i.e., along the upper edge of Figures 4–7) are indicative of the pattern of larger and smaller hillslopes. Concavity represents a landscape that trends to larger hillslopes and greater upland convergence, with the reverse true for convexity. The relative change in thickness of the color bands indicates the degree of loss to groundwater at that point in the watershed network. For a given source location, a greater pinching of the thickness of its color band corresponds to more significant loss of that water to groundwater. The combination of these shapes (concavities/convexities in the increase of discharge and the pinching of the color bands representing distinct spatial sources) represents the intersection of hydrologic turnover with watershed structure/network geometry and is illustrated simply in these synthetic watersheds.

4.1.2. Natural Watersheds

Discharge accumulation patterns in natural watersheds (Figure 7) consist of complex arrangements of the simpler shapes exhibited by the synthetic watersheds. These nested patterns mirror the well-documented fractal patterns of watershed structure and stream network geometry in natural watersheds [i.e., *Tarboton et al.*, 1988]. Concavities at any scale represent increasing accumulation of area moving downstream, indicative of either more convergent hillslopes or a higher density of stream reaches at those network distances. Likewise, source compositions in each of these watersheds evolve with distinct patterns that are complex combinations of the simpler ones exhibited by synthetic examples (Figures 5 and 6). Steeper slopes between color bands at a given network distance represent greater losses and therefore greater hydrologic turnover.

Source compositions at the outlet of each watershed are in part a reflection of the distributions of local inputs along the network, but the two become increasingly decoupled moving further away from the outlet. Inputs to the stream network that have traveled through more reaches are increasingly diminished relative to the corresponding distribution of LI (gray bars, Figure 8). This decoupling indicates that more distal sources are diminished while more proximal sources are relatively magnified in their contribution to source compositions at the outlet. Despite the noticeable differences in the patterns and evolution of source compositions and their relationship to the unique morphologies of each watershed, it is important to note similarities in these patterns amongst watersheds. Each distinct source generally exhibits an exponential decline in contribution moving downstream, as is required by the form of equation (7). Although the shape of the decline varies with the magnitude of each LI, the general shape remains the same. This results in similar weighting of watershed outlet source compositions toward sources closer to watershed outlets (Figures 4b and 5–7). This weighting is illustrated further in the relative magnification of the contribution to outlet source compositions from more proximal locations (Figure 8). Therefore, closer locations can have a greater influence on outlet source compositions while more distant inputs are diminished and exert much less influence than the magnitude of the input alone might suggest.

These similarities between watersheds can facilitate a general understanding of how stream networks can modify watershed signals. However, we found no discernable trend in these patterns related to simple, aggregated watershed metrics (e.g., Horton's form factor, circularity, etc.). This emphasizes the value of understanding hydrologic turnover in a spatially distributed manner that maintains the topology of the reach-to-reach processes. We suggest that this or similar modeling approaches represent valuable and potentially the only method at this time of estimating watershed signal modification due to hydrologic turnover.

4.2. What Are the Implications of Stream Network Scale Hydrologic Turnover for Interpreting Watershed Processes in Stream Signals?

In the absence of hydrologic turnover the spatial distribution of local inputs could serve as a surrogate for source compositions and therefore the relative influence that each location has on watershed outlet signals. In this case, stream network positions with highly convergent or large hillslopes or with a higher density of stream reaches would therefore have a larger influence on watershed outlet source compositions regardless of position within the stream network (Figure 4a). However, hydrologic turnover at the network scale modifies these signals such that the spatial location of a LI also influences its impact on downstream source compositions. Because of longitudinally compounded hydrologic turnover, an input's influence downstream depends on the magnitude of the input but is also weighted by the amount of hydrologic turnover that has occurred downstream through the stream network. Since further distance traveled in the stream network subjects an input to greater hydrologic turnover, in general greater distance traveled by an input corresponds to a decreased influence on source compositions relative to one that has traveled less distance. Because of this stream network influence on stream source compositions, it is requisite to understand spatial distributions of hydrologic turnover, among other hydrological and biogeochemical processes, for interpreting observed stream signals as the convolution of terrestrial watershed and stream network processes. This interpretation can be challenging in natural watersheds. It is therefore instructive to consider how these complex watersheds are in fact arrangements of much simpler shapes similar to the synthetic watersheds presented herein (Figures 5 and 6).

Hydrologic turnover results in the mixing of solutes between hydrologic reservoirs with distinct biogeochemical signatures. Although this general principle has been applied in numerous stream studies [e.g., *Bencala*, 1993; *McKnight and Bencala*, 1990; *Zarnetske et al*., 2011], the simultaneous gains and losses that characterize hydrologic turnover have not been incorporated in these previous examples. Improving this understanding and representation of the spatial distribution of hydrologic turnover is valuable to understanding spatial patterns of solute and stream water signatures. Hydrologic turnover can influence the concentrations of nutrients or other solutes that are endogenous to the watershed, and can also exert an attenuating effect on solutes (i.e., pollutants) that are introduced to the watershed. Interaction between groundwater and stream water can act to retain solutes from the stream and dilute the remaining with groundwater. When considering hydrologic turnover and its implications for pollutant transport through a stream network one can consider the turnover factor (*TF*, equation (5)) as an impact factor. At each stream reach the turnover factor reflects the impact that groundwater exchange exerts on in-stream solute concentrations or signatures. With extension to

multiple reaches, it is the serial combination of these impact factors which influences the retention, transport, and concentration of solutes introduced to the watershed from exogenous sources.

We believe that this analysis includes the minimum watershed information necessary for a first approximation of the processes described herein across the landscape. The relationship presented here (Figure 2b) was stable across the landscape positions and at different flow states, and we additionally observed the opposite relationship with gross loss, with greater losses occurring at higher flow states. This emphasizes the effectiveness of this measurement technique. Although gross volumteric losses were measured to be higher at higher flows (potentially due to higher wetted channel perimeter), they had markedly less influence on streamflow than at lower flows. Although the trend observed was less pronounced, similar dynamics were reported in *Payn et al*. [2009]. A less clear relationship in that study could relate to the shorter reaches used, the sharp geologic transition reported in that study, or the more heterogeneous, landscape of the Tenderfoot Creek Experimental Forest when compared to the glacially formed Sawtooth watersheds.

We assumed a stream network in hydrological equilibrium with its watershed, an assumption justified by the short term stability of hydrographs in arid, snowmelt-dominated watersheds during base flow. Relaxation of this assumption makes the analysis more challenging to interpret, but a logical next step would be to apply it in watersheds exhibiting nonstationarity over time scales shorter than the time scales of stream transport. Under nonstationary conditions, we speculate that the patterns of source composition (color bands, Figures 4–7) would shift from more representative of the lateral input structure (Figure 8, gray bars) at higher flows to exhibiting stronger effects of hydrologic turnover at lower flows. This is due to moderately increasing absolute losses to groundwater relative to strongly increasing fluxes of water downstream at higher flows [*Covino et al*., 2011]. Therefore, smaller percent losses to groundwater at higher flows would lead to stronger lateral input signal preservation during periods of higher streamflow.

The specific relationships presented here (Figure 2) are unique to these watersheds, but the general relationships and conceptual model could be widely applicable in a variety of watersheds. Other watersheds in distinct geoclimatic settings may exhibit relationships between hydrologic turnover and stream slope, bed materials, hydraulic radius, stream velocity, or other geomorphic or hydrologic characteristics. In these cases, one would merely need to substitute locally appropriate relationships into the same analytical framework. If no simple relationships are apparent, direct measurement [i.e., *Payn et al*., 2009] or statistical sampling of a hypothesized distribution could be performed to either directly characterize network scale hydrology or explore the potential range of effects at that scale, respectively.

To date, this simple modeling framework has treated the loss of stream water to groundwater as one-way and has not yet considered how some appreciable and variable fraction of lateral gains could be composed of upstream or previous local losses. Although this is a likely scenario, this process cannot be directly measured using existing tracer tools. Therefore, in this analysis, we refer to the source of stream water as the most recent spatial location of water entering the stream network and consequently its most recent biogeochemical setting. The key message is that hydrologic turnover can lead to shifting source composition of water such that it becomes increasingly decoupled from the structure of the lateral gains to the stream network. Our conceptual and numerical model highlights this process and focuses on how turnover propagates through stream networks given the field experimental constraints of today's instruments and methods. Implementing the return of previous losses to stream water and associated (potentially modified) solutes is a logical next step. Initially, this could be explored with virtual or statistical experiments until new tracer technology and methods become available.

The stream network is an intermediate between terrestrial biological, chemical, or ecological signals at the watershed scale and their influence on some integrated stream signal at a downstream sampling location. As such, whether inferring terrestrial watershed processes from stream signals or predicting the effect of observed terrestrial processes on stream signals, it is paramount to understand the degree to which each source influences the stream water composition observed at a given spatial location. Our results suggest that in order to interpret stream signals as reflections of watershed terrestrial processes or to predict the effects of terrestrial processes on streams it can be critical to characterize the spatial distribution of hydrologic turnover and the resulting source compositions. This becomes particularly important in cases where the terrestrial processes of interest are distributed heterogeneously across watersheds. Resulting variable stream network loading could then be modified by the stream network in a manner unique to each

watershed and stream network. Thus, the stream network can be conceptualized as a filter through which spatially heterogeneous watershed signals are both integrated and modified, resulting in signals propagated downstream that are a convolution of terrestrial inputs and stream processes. We suggest that the deconvolution of these stream signals to directly infer watershed processes can be intractable without characterization of the hydrologic processes that occur within stream networks.

5. Conclusion

We expand here on a method we initially proposed in *Covino et al*. [2011] for elucidating how stream networks can modify watershed signals through hydrologic turnover (the simultaneous or sequential gain and loss of stream water from and to groundwater, respectively). *Covino et al*. [2011] presented measured hydrologic turnover (gross gains and losses) at the stream reach scale and related these observed hydrologic dynamics to hydrologic (stream discharge, *Q*) and terrain (local input area, *LI*) metrics that could be used to scale these measurements from reaches to watersheds. We expanded on this proof-of-concept by simulating hydrologic turnover across seven synthetic (11–15 km^2) and six natural (11–64 km^2) watersheds to elucidate how stream network geometry and watershed structure modify source compositions observed across stream networks.

We observed that the contribution to discharge from any one upstream source was initially controlled by the local hillslope size (i.e., the size of the input). However, this contribution diminished as it moved downstream due to compounded hydrologic turnover. The result of this compounded turnover was that stream source compositions were weighted toward proximal inputs rather than toward larger inputs. We documented a progressive decoupling, increasing farther downstream toward the outlet, of watershed outlet source composition from the distribution of local inputs. The evolution of source compositions in each watershed is distinct, illustrating the importance of watershed structure and stream network geometry in controlling specific spatial patterns of evolution of source compositions. Our results suggest that the influence of a given local input on stream signals is dependent on the magnitude of the initial input and the degree of hydrologic turnover has undergone, with the latter becoming increasingly important as a function of greater distance traveled in the network. These results emphasize the role of the stream network in modifying watershed signals from hillslope inputs.

In summary: (1) hydrologic turnover is the result of variable gains and losses across stream networks; (2) hydrologic turnover varies spatially due to heterogeneous local inputs throughout the network, which are organized by both watershed structure and stream network geometry; (3) network-scale turnover can be characterized by a spatially distributed method that accounts for internal watershed organization; (4) distributed modeling of hydrologic turnover reveals the variability in source compositions that can result from distinct watershed structures and network geometries; and (5) we elucidate how hydrologic turnover generally modifies hydrologic systems such that the original spatial structure of lateral inputs to the stream network is convoluted with compounded hydrologic turnover moving downstream. Because the stream network can act as a filter to modify watershed signals, understanding network-scale hydrologic turnover is important both for predicting how watershed signals are manifested in their stream networks and for interpreting stream signals as convolutions of stream and watershed processes.

Acknowledgments
Financial support was provided by a grant from the National Science Foundation DEB-0519264, EAR 0943640, and EAR 0337650. We would like to thank Brian Iacona, Kelly Conde, Malcolm Herstand, and Alexey Kalinin for assistance with fieldwork and the Boise National Forest for allowing access to sampling sites. We would also like to thank Anna Bergstrom for research support including terrain analysis and both Ryan Emanuel and Lucy Marshall for fruitful discussions and feedback.

References

Agnese, C., D. D'asaro, and G. Giordano (1988), Estimation of the time scale of the geomorphologic instantaneous unit hydrograph from effective streamflow velocity, *Water Resour. Res.*, *24*, 969–978.
Anderson, M. G., and T. P. Burt (1978), The role of topography in controlling throughflow generation, *Earth Surf. Processes*, *3*(4), 331–344.
Bencala, K. E. (1993), A perspective on stream-catchment connections, *J. North Am. Benthol. Soc.*, *12*, 44–47.
Bencala, K. E., and R. A. Walters (1983), Simulation of solute transport in a mountain pool-and-riffle stream: A transient storage model, *Water Resour. Res.*, *193*, 718–724.
Bencala, K. E., M. N. Gooseff, and B. A. Kimball (2011), Rethinking hyporheic flow and transient storage to advance understanding of stream-catchment connections, *Water Resour. Res.*, *47*, W00H03, doi:10.1029/2010WR010066.
Benettin, P., Y. van der Velde, S. E. A. T. M. van der Zee, A. Rinaldo, and G. Botter (2013a), Chloride circulation in a lowland catchment and the formulation of transport by travel time distributions, *Water Resour. Res.*, *49*, 4619–4632, doi:10.1002/wrcr.20309.
Benettin, P., A. Rinaldo, and G. Botter (2013b), Kinematics of age mixing in advection-dispersion models, *Water Resour. Res.*, *49*, 8539–8551, doi:10.1002/2013WR014708.
Beven, K. J., and M. J. Kirkby (1979), A physically based, variable contributing area model of basin hydrology, *Hydrol. Sci. J.*, *24*, 43–69.
Bormann, F. H., and G. E. Likens (1967), Nutrient cycling, *Science*, *155*, 424–429.
Botter, G., and A. Rinaldo (2003), Scale effect on geomorphologic and kinematic dispersion, *Water Resour. Res.*, *39*(10), 1286, doi:10.1029/2003WR002154.

Botter, G., F. Peratoner, M. Putti, A. Zuliani, R. Zonta, A. Rinaldo, and M. Marani (2008), Observation and modeling of catchment-scale solute transport in the hydrologic response: A tracer study, *Water Resour. Res.*, *44*, W05409, doi:10.1029/2007WR006611.
Briggs, M. A., M. N. Gooseff, B. J. Peterson, K. Morkeski, W. M. Wollheim, and C. S. Hopkinson (2010), Surface and hyporheic transient storage dynamics throughout a coastal stream network, *Water Resour. Res.*, *46*, W06516, doi:10.1029/2009WR008222.
Cardenas, M. B. (2008), Surface water-groundwater interface geomorphology leads to scaling of residence times, *Geophys. Res. Lett.*, *35*, L08402, doi:10.1029/2008GL033753.
Covino, T. P., and B. L. McGlynn (2007), Stream gains and losses across a mountain to valley transition: Impacts on watershed hydrology and stream water chemistry, *Water Resour. Res.*, *43*, W10431, doi:10.1029/2006WR005544.
Covino, T. P., B. L. McGlynn, and M. A. Baker (2010), Separating physical and biological nutrient retention and quantifying uptake kinetics from ambient to saturation in successive mountain stream reaches, *J. Geophys. Res.*, *115*, G04010, doi:10.1029/2009JG001263.
Covino, T. P., B. L. McGlynn, and J. M. Mallard (2011), Stream-groundwater exchange and hydrologic turnover at the network scale, *Water Resour. Res.*, *47*, W12521, doi:10.1029/2011WR010942.
D'Odorico, P., and R. Rigon (2003), Hillslope and channel contributions to the hydrologic response, *Water Resour. Res.*, *39*(5), 1113, doi:10.1029/2002WR001708.
Emanuel, R. E., A. G. Hazen, B. L. McGlynn, and K. G. Jencso (2014), Vegetation and topographic influences on the connectivity of shallow groundwater between hillslopes and streams, *Ecohydrol.*, *7*, 887–895, doi:10.1002/eco.1409.
Ensign, S. H., and M. W. Doyle (2006), Nutrient spiraling in streams and river networks, *J. Geophys. Res.*, *111*, G04009, doi:10.1029/2005JG000114.
Findlay, S. (1995), Importance of surface-subsurface exchange in stream ecosystems: The hyporheic zone, *Limnol. Oceanogr.*, *40*(1), 159–164.
Fisher, H. B., E. J. List, R. C. Y. Koh, J. Imberger, and N. H. Brooks (1979), *Mixing in Inland and Coastal Waters*, Academic, San Diego, Calif.
Fisher, S. G., R. A. Sponseller, and J. B. Hefferman (2004), Horizons in stream biogeochemistry: Flowpaths to progress, *Ecology*, *85*, 2369–2379.
Grabs, T., K. J. Jencso, B. L. McGlynn, and J. Seibert (2010), Calculating terrain indices along streams—A new method for separating stream sides, *Water Resour. Res.*, *46*, W12536, doi:10.1029/2010WR009296.
Gupta, V. K., E. Waymire, and C. T. Wang (1980), A representation of an instantaneous unit hydrograph from geomorphology, *Water Resour. Res.*, *16*, 855–862.
Harvey, J. W., B. J. Wagner, and K. E. Bencala (1996), Evaluating the reliability of the stream tracer approach to characterize stream-subsurface water exchange, *Water Resour. Res.*, *32*, 2441–2451.
Hill, A. R. (1990), Groundwater flow paths in relation to nitrogen chemistry in the near-stream zone, *Hydrobiologia*, *206*, 39–52.
Horton, R. (1932), Drainage-basin characteristics, *Trans. AGU*, *13*, 350–361.
Hrachowitz, M., C. Soulsby, D. Tetzlaff, J. J. C. Dawson, S. M. Dunn, and I. A. Malcolm (2009), Using long-term data sets to understand transit times in contrasting headwater catchments, *J. Hydrol.*, *367*(3–4), 237–248.
Jencso, K. G., B. L. McGlynn, M. N. Gooseff, S. M. Wondzell, K. E. Bencala, and L. A. Marshall (2009), Hydrologic connectivity between landscapes and streams: Transferring reach- and plot-scale understanding to the catchment scale, *Water Resour. Res.*, *45*, W04428, doi:10.1029/2008WR007225.
Jencso, K. J., and B. L. McGlynn (2011), Hierarchical controls on runoff generation: Topographically driven hydrologic connectivity, geology, and vegetation, *Water Resour. Res.*, *47*, W11527, doi:10.1029/2011WR010666.
Kalbus, E., F. Reinstorf, and M. Schirmer (2006), Measuring methods for groundwater—Surface water interactions: A review, *Hydrol. Earth Syst. Sci.*, *10*, 873–887.
Kiilsgaard, T., L. Stanford, and R. Lewis (2003), *Preliminary Geologic Map of the Northeast Part of the Deadwood River 30.60 Minute Quadrangle, Idaho*, Idaho Geol. Surv., Moscow.
Kilpatrick, F. A., and E. D. Cobb (1985), Measurement of discharge using tracers, report of the U.S. Geological Survey, *U.S. Geol. Surv. Tech. Water Resour. Invest., Book 3, Chap. A16*, 6–15.
Kirchner, J. W. (2009), Catchments as simple dynamical systems: Catchment characterization, rainfall-runoff modeling, and doing hydrology backward, *Water Resour. Res.*, *45*, W02429, doi:10.1029/2008WR006912.
Kirchner, J. W., X. Feng, and C. Neal (2000), Fractal stream chemistry and its implications for contaminant transport in catchments, *Nature*, *403*, 524–527.
Kirchner, J. W., X. Feng, and C. Neal (2001), Catchment-scale advection and dispersion as a mechanism for fractal scaling in stream tracer concentrations, *J. Hydrol.*, *254*, 81–100.
Kirkby, M. (1976), Tests of random network model, and its application to basin hydrology, *Earth Surf. Processes*, *1*(3), 197–212.
Lee, M. T., and J. W. Delleur (1976), A variable source area model of the rainfall-runoff process based on the watershed stream network, *Water Resour. Res.*, *12*, 1029–1036.
Leopold, L., and T. Maddock (1953), The hydraulic geometry of stream channels and some physiographic implications, *U.S. Geol. Surv. Prof. Pap., 282-A*.
Leopold, L. B., M. G. Wolman, and J. P. Miller (1964), *Fluvial Processes in Geomorphology*, 522 pp., Freeman, San Francisco, Calif.
MccLain, M. E., et al. (2003), Biogoechemical hot spots and hot moments at the interface of terrestrial and aquatic ecosystems, *Ecosystems*, *6*, 301–312.
McDonnell, J. J., M. K. Stewart, and I. F. Owens (1991), Effect of catchment-scale subsurface mixing on stream isotopic response, *Water Resour. Res.*, *27*, 3065–3073.
McGlynn, B. L., and J. Seibert (2003), Distributed assessment of contributing area and riparian buffering along stream networks, *Water Resour. Res.*, *39*(4), 1082, doi:10.1029/2002WR001521.
McGlynn, B. L., J. J. McDonnell, J. Seibert, and C. Kendall (2004), Scale effects on headwater catchment runoff timing, flow sources, and groundwater-streamflow relations, *Water Resour. Res.*, *40*, W07504, doi:10.1029/2003WR002494.
McGuire, K. J., and J. J. McDonnell (2006), A review and evaluation of catchment transit time modeling, *J. Hydrol.*, *330*(3–4), 543–563.
McGuire, K. J., J. J. McDonnell, M. Weiler, C. Kendall, B. L. McGlynn, J. M. Welker, and J. Seibert (2005), The role of topography on catchment-scale water residence time, *Water Resour. Res.*, *41*, W05002, doi:10.1029/2004WR003657.
McKnight, D. M., and K. E. Bencala (1990), The chemistry of iron, aluminum, and dissolved organic material in three acidic, metal-enriched, mountain streams, as controlled by watershed and in-stream processes, *Water Resour. Res.*, *26*, 3087–3100.
Mesa, O. J., and E. R. Mifflin (1986), On the relative role of hillslope and network geometry in hydrologic response, in *Scale Problems in Hydrology*, edited by V. K. Gupta, I. Rodriguez-Iturbe, and E. F. Wood, 1–17, D. Reidel, Norwell, Mass.

Mulholland, P. J., and D. L. DeAngelis (2000), Chapter 6: Surface-subsurface exchange and nutrient spiraling, in *Streams and Ground Waters*, edited by J. A. Jones and P. J. Mulholland, pp. 149–166, Academic, San Diego, Calif.
Mulholland, P. J., et al. (2008), Stream denitrification across biomes and its response to anthropogenic nitrate loading, *Nature*, *452*, 202–205.
Naden, P. S. (1992), Spatial variability in flood estimation for large catchments: The exploitation of channel network structure, *J. Hydrol. Sci.*, *37*, 53–71.
Nippgen, F., B. L. McGlynn, L. Marshall, and R. Emanuel (2011), Landscape structure and climatic influences on hydrologic response, *Water Resour. Res.*, *47*, W12528, doi:10.1029/2011WR011161.
O'Callaghan, J., and D. Mark (1984), The extraction of drainage networks from digital elevation data, *Comput. Vision Graph. Image Process.*, *28*(3), 323–344.
Olaya, V. (2004), *A gentle introduction to SAGA GIS, User manual*, The SAGA User Group e.V, Gottingen.
Payn, R. A., M. N. Gooseff, B. L. McGlynn, K. E. Bencala, and S. M. Wondzell (2009), Channel water balance and exchange with subsurface flow along a mountain headwater stream in Montana, United States, *Water Resour. Res.*, *45*, W11427, doi:10.1029/2008WR007644.
Rinaldo, A., G. K. Vogel, R. Rigon, and I. Rodriguez-Iturbe (1995), Can One Gauge the Shape of a Basin?, *Water Resour. Res.*, *31*(4), 1119–1127, doi:10.1029/94WR03290.
Rinaldo, A., R. Rigon, and A. Marani (1991), Geomorphological dispersion, *Water Resour. Res.*, *27*(4), 513–525.
Rinaldo, A., K. J. Beven, E. Bertuzzo, L. Nicotina, J. Davies, A. Fiori, D. Russo, and G. Botter (2011), Catchment travel time distributions and water flow in soils, *Water Resour. Res.*, *47*, W07537, doi:10.1029/2011WR010478.
Roberts, B. J., and P. J. Mulholland (2007), In-stream biotic control on nutrient biogeochemistry in a forested stream, West Fork of Walker Branch, *J. Geophys. Res.*, *112*, G04002, doi:10.1029/2007JG000422.
Robinson, J. S., M. Sivapalan, and J. D. Snell (1995), On the relative roles of hillslope processes, channel routing, and network geomorphology in the hydrologic response of natural catchments, *Water Resour. Res.*, *31*, 3089–3101.
Rodriguez-Iturbe, I., and J. Valdes (1979), Geomorphologic structure of hydrologic response, *Water Resour. Res.*, *15*, 1409–1420.
Ruehl, C., A. T. Fisher, C. Hatch, M. Los Huertos, G. Stemler, and C. Shennan (2006), Differential gauging and tracer tests resolve seepage fluxes in a strongly losing stream, *J. Hydrol.*, *330*, 235–248.
Runkel, R. (2002), A new metric for determining the importance of transient storage, *J. North Am. Benthol. Soc.*, *21*, 529–543.
Saco, P. M., and P. Kumar (2002a), Kinematic dispersion in stream networks, 1, Coupling hydraulic and network geometry, *Water Resour. Res.*, *38*(11), 1244, doi:10.1029/2001WR000695.
Saco, P. M., and P. Kumar (2002b), Kinematic dispersion in stream networks, 2, Scale issues and self-similar network organization, *Water Resour. Res.*, *38*(11), 1245, doi:10.1029/2001WR000694.
Saco, P. M., and P. Kumar (2004), Kinematic dispersion effects of hillslope velocities, *Water Resour. Res.*, *40*, W01301, doi:10.1029/2003WR002024.
Sebestyen, S. D., E. W. Boyer, J. B. Shanley, C. Kendall, D. H. Doctor, G. R. Aiken, and N. Ohte (2008), Sources, transformations, and hydrological processes that control stream nitrate and dissolved organic matter concentrations during snowmelt in an upland forest, *Water Resour. Res.*, *44*, W12410, doi:10.1029/2008WR006983.
Seibert, J., and B. L. McGlynn (2007), A new triangular multiple flow direction algorithm for computing upslope areas from gridded digital elevation models, *Water Resour. Res.*, *43*, W04501, doi:10.1029/2006WR005128.
Sherman, L. K. (1932), Streamflow from rainfall by the unit hydrograph method, *Eng. News Rec.*, *108*, 501–505.
Snell, J. D., and M. Sivapalan (1994), On geomorphological dispersion in natural catchments and the geomorphological unit hydrograph, *Water Resour. Res.*, *30*, 2311–2323.
Soulsby, C., R. Malcolm, R. C. Ferrier, R. C. Helliwell, and A. Jenkins (2000), Isotope hydrology of the Allt a'Mharcaidh catchment, Cairngorms, Scotland: Implications for hydrological pathways and residence times, *Hydrol. Processes*, *14*, 747–762.
Stanford, J. A., and J. V. Ward (1993), An ecosystem perspective of alluvial rivers: Connectivity and the hyporheic corridor, *J. North Am. Benthol. Soc.*, *12*, 48–60.
Tarboton, D. G., R. L. Bras, and I. Rodriguez-Iturbe (1988), The fractal nature of river networks, *Water Resour. Res.*, *24*, 1317–1322.
Tetzlaff, D., J. Seibert, K. J. McGuire, H. Laudon, D. A. Burns, S. M. Dunn, and C. Soulsby (2009), How does landscape structure influence catchment transit time across different geomorphic provinces?, *Hydrol. Processes*, *23*, 945–953.
Uhlenbrook, S., M. Frey, C. Leibundgut, and P. Maloszewski (2002), Hydrograph separations in a meso-scale mountainous basin at event and seasonal timescales, *Water Resour. Res.*, *38*(6), 1096, doi:10.1029/2001WR000938.
van der Tak, L. D., and R. L. Bras (1990), Incorporating hillslope effects into the geomorphologic instantaneous unit hydrograph, *Water Resour. Res.*, *26*, 2393–2400.
van der Velde, Y., P. J. J. F. Torfs, S. E. A. T. M. van der Zee, and R. Uijlenhoet (2012), Quantifying catchment-scale mixing and its effect on time-varying travel time distributions, *Water Resour. Res.*, *48*, W06536, doi:10.1029/2011WR011310.
Vannote, R. L., G. W. Minshall, K. W. Cummins, J. R. Sedell, and C. E. Gushing (1980), The river continuum concept, *Can. J. Fish. Aquat. Sci.*, *37*, 130–137.
Wagner, B. J., and J. W. Harvey (1997), Experimental design for estimating parameters of rate-limited mass transfer: Analysis of stream tracer studies, *Water Resour. Res.*, *33*, 1731–1741.
Ward, A. S., R. A. Payn, M. N. Gooseff, B. L. McGlynn, K. E. Bencala, C. A. Kelleher, S. M. Wondzell, and T. Wagener (2013), Variations in surface water-ground water interactions along a headwater mountain stream: Comparisons between transient storage and water balance analyses, *Water Resour. Res.*, *49*, 3359–3374, doi:10.1002/wrcr.20148.
Weiler, M., B. L. McGlynn, K. J. McGuire, and J. J. McDonnell (2003), How does rainfall become runoff?, A combined tracer and runoff transfer function approach, *Water Resour. Res.*, *39*(11), 1315, doi:10.1029/2003WR002331.
Wondzell, S. M. (2011), The role of the hyporheic zone across stream networks, *Hydrol. Processes*, *25*, 3525–3532.
Woods, R. A., and M. Sivapalan (1997), A connection between topographically driven runoff generation and channel network structure, *Water Resour. Res.*, *33*, 2939–2950.
Yen, B. C., and K. T. Lee (1997), Unit hydrograph derivation for ungaged watersheds by stream order laws, *J. Hydrol. Eng.*, *2*(1), 1–9.
Zarnetske, J. P., R. Haggerty, S. M. Wondzell, and M. A. Baker (2011), Dynamics of nitrate production and removal as a function of residence time in the hyporheic zone, *J. Geophys. Res.*, *116*, G01025, doi:10.1029/2010JG001356.